10th International Conference on Composite Science and Technology
ICCST/10
A.L. Araújo, J.R. Correia, C.M. Mota Soares, et al. (Editors)

EVALUATION ON MECHANICAL BEHAVIOUR OF NEW ODS ALLOYS

Bohuslav Masek[*], Omid Khalaj[*], Hana Jirkova[*], Jiri Svoboda[†]

[*] Research Centre of Forming Technology, FORTECH, University of West Bohemia
Univerzitní 22, 306 14, Pilsen, Czech Republic
khalaj@vctt.zcu.cz

[†] Institute of Physics of Materials, Academy of Sciences Czech Republic
Zizkova 22, 616 62, Brno, Czech Republic
svobj@ipm.cz

Key words: ODS steel, alloys, Fe-Al.

Summary: *It is possible to gain new unconventional types of structures with specific mechanical properties by combining of various types of materials and technologies. One of the possibilities is enabled by a combination of powder metallurgy with hot consolidation. The powder of metal matrix with dispersed stable particles achieved by mechanical alloying is consolidated by hot rolling. For production of intricately shaped components from such materials, new processes must be found to allow near net shape products to be manufactured in a simple and rapid manner. The main motivation of this paper is to evaluate the mechanical properties of new Oxide Dispersion Strengthened (ODS) Fe-Al based alloys applicable at high temperatures up to about 1100°C. To find out the influence of the temperature on the microstructure, several thermomechanical treatments at temperatures between 30°C and 1200°C with specific deformation profiles were performed.*

1 INTRODUCTION

The specific mechanical property and structure of the material could be achieved by combining various types of materials and technologies. One of these possibilities is to prepare composites by combination of powder metallurgy with hot consolidation. A potential group of structural materials for high temperature creep applications are Oxide Dispersion Strengthened (ODS) alloys.

The ODS alloys commercially produced in the end of the 20th century and the begin of the 21th century are represented by MA 956 or MA957 [1], PM 2000 or PM 2010 [2], ODM alloys [3] and 1DK or 1DS [4] with ferritic matrix by ODS Eurofer steels with tempered ferritic-martensitic matrix [5] and by austenitic Ni-ODS PM 1000 or Ni-ODS PM 3030 [6]. The volume fraction of dispersed spherical oxides (usually Y_2O_3) is typically below 1 % and the oxides are typically of a mean size of 5-30 nm. Because of the lower diffusion coefficient austenitic ODS alloys show a better creep resistance for the same oxide volume fraction and contain some minimum chromium and/or aluminium content to guarantee sufficient oxidation resistance. However, the resistance to the coarsening of oxides (and thus stability of creep properties) is given by the product of the solubility of oxygen in the matrix and its diffusion coefficient [7]; this factor is more advantageous for ferritic ODS alloys. That is

probably the reason, why the application of ferritic ODS steels dominate. The excellent creep properties of the ODS alloys are due to attractive interaction of dislocations with oxides described in the well-known model by Rösler and Arzt [8]. Creep usually exhibits a threshold stress, which correlates well with the Orowan theory predicting that at a given temperature the threshold stress is inversely proportional to the distance of the oxides. Thus, any coarsening of oxides causes the degradation of creep properties. Typical creep strength of the ferritic ODS alloys is estimated in the open literature as 60 (40) MPa for coarse-grained structures and 20 (6) MPa for fine-grained structures at 1000 (1100) °C [9]. Additional ODS ferritic steels are currently in development at Oak Ridge National Laboratories [10-13]. A sufficient content of Al and/or Cr in the ODS alloy is decisive for its oxidation resistance.

The new ODS and alloys and composites consist of a ferritic Fe-Al matrix strengthened with about 6 to 10 vol. % of Al_2O_3 particles. An experimental program was carried out in order to get a more detailed insight into these new groups of materials, to better understand their processing behavior and their operational properties.

2 EXPERIMENTAL PROCEDURE

Mechanically alloyed powders were prepared in a low energy ball mill developed by the authors (Figure 1). It enables evacuation and filling by Oxygen gas. It has two steel containers (each 24 l) and each container was filled by 80 steel balls of diameter 40 mm. A variable revolution speed is between 20 rpm to 75 rpm.

The mechanically alloyed powders consisting of Fe10wt%Al matrix and 6 to 10vol.% of Al_2O_3 particles were deposited into a steel container of diameter 70 mm, evacuated and sealed by welding. The steel container was heated up to temperature of 900ºC and rolled by a hot rolling mill (Figure 2) to the thickness of 25 mm in the first rolling step and than heated up to temperature of 1100ºC and rolled to the thickness of 9 mm in the second step. A 6 mm thick sheet of the ODS alloy was produced in this way. The specimens were cut by water jet.

Figure 1: Low energy mill for mechanical alloying

Figure 2: Hot Rolling Mill

In order to investigate the thermomechanical treatment of specimens, a thermomechanical simulator (Figure 3) was used, which allows running of various temperature-deformation paths necessary for finding conditions leading e.g. to the most effective grain coarsening by recrystallization. Several procedures of thermomechanical treatment were designed and carried out yet, which differed in the number of deformation steps characterized by different strains, strain rates and temperatures. The thermomechanical simulator also allows combination of tensile and compressive deformation, thus accumulating a high plastic deformation (and a high dislocation density) in the specimen.

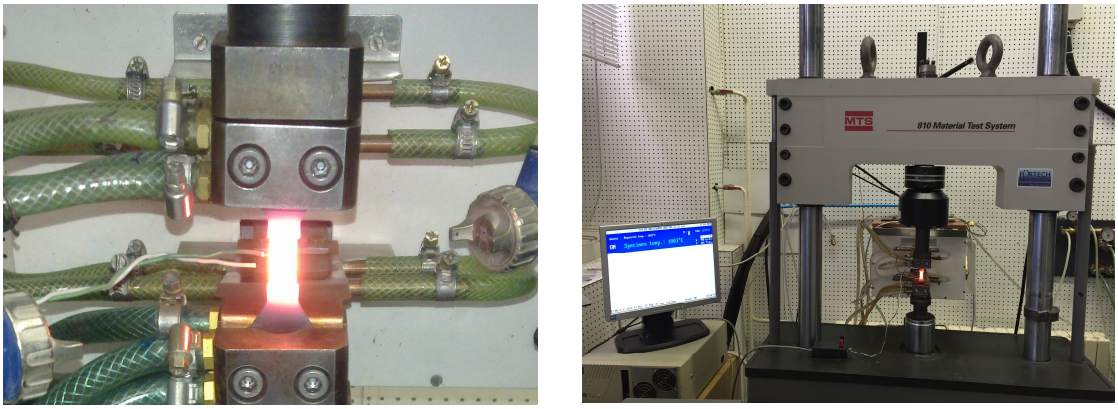

Figure 3: Thermomechanical Simulator

3 SPECIMEN PREPARATION

Two forms of specimens (Figure 4) were selected out of several forms regarding to their most homogeneous temperature fields. After the specimens were cut water jet they where grinded before testing.

Four types of material were used in this research as described in Table 1. All types of materials are based on Fe10wt%Al ferritic matrix with different particle size and Vol.% of Al_2O_3. An Al_2O_3 powder was added to prepare the composite, fine oxides in ODS alloys have been created by internal oxidation during mechanical alloying and precipitated during hot consolidation. The microscopic SEM observations indicated several inhomogeneities due to sticking of the material during mechanical alloying on the walls of the milling container. These inhomogeneities can also influence the mechanical and fracture properties of the material but the mechanical alloying process is steadily optimized with respect to homogeneity of the materials.

Material No.	Material Type	Milling time (hours)	Ferritic Matrix	Vol.% of Al_2O_3	Typical Particle Size (nm)
1	Composite	--	Fe10wt%Al	10	300
2	ODS Alloy	100	Fe10wt%Al	6	50-200
3	ODS Alloy	150	Fe10wt%Al	6	50-150
4	ODS Alloy	200	Fe10wt%Al	6	30-150

Table 1: Material Properties

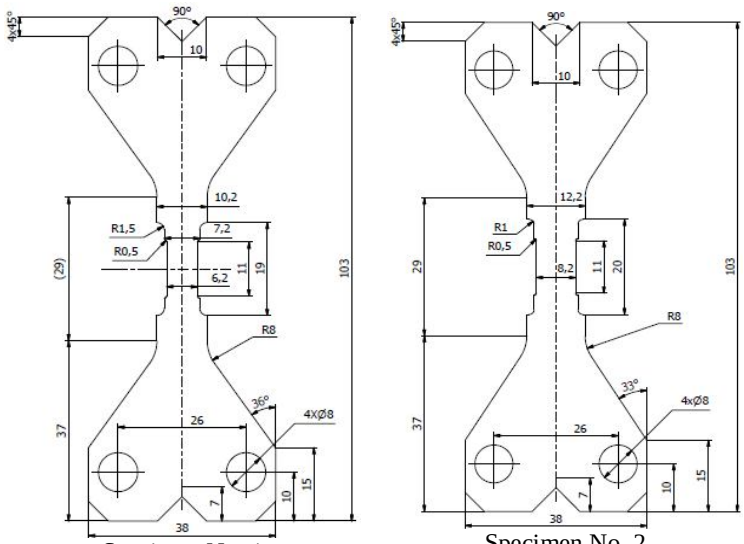

Figure 4: Specimen's dimensions

4 TESTING PROGRAM

The test program was divided into different series. Tests are summarized in Table 2.

Test Series	Material No.	Specimen Shape No.	Treatment No.	Maximum Temperature (ºC)	Number of Tests	Purpose of Tests
A	1	1, 2	1	1150	2	To check the temperature field
B	1	1, 2	2	1150, 750, 30	6	To check the specimen shape effect
C	1	2	2	1200, 1100, 1000, 900, 800, 30	6	To check the material thermomechanical behaviour
D	2	2	2		6	
E	3	2	2		6	
F	4	2	2		6	

Table 2: Parameters of test program

Test series A was carried out to check the temperature field with the desired material 1. As Figure 5 shows, the temperature is raised to 1150ºC during 3 minutes, is stable for 3 minutes and then falls down to room temperature over 3 minutes (treatment number 1).

Test series B was performed to check the material behaviour under treatment number 2 (Figure 6). In this case, two specimen shapes were tested at three different temperatures to determine the behaviour of this composite material 1.

Test series C to F were carried out to investigate the thermomechanical behaviour of the different material (1 to 4) at different temperatures more precisely. In order to have a better demonstration of the results comparison, only the results at RT, 800 ºC and 1200 ºC are presented.

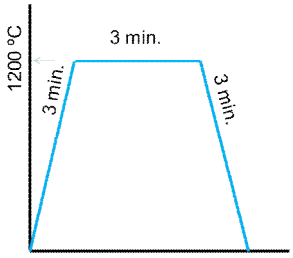

Figure 5: Treatment No. 1

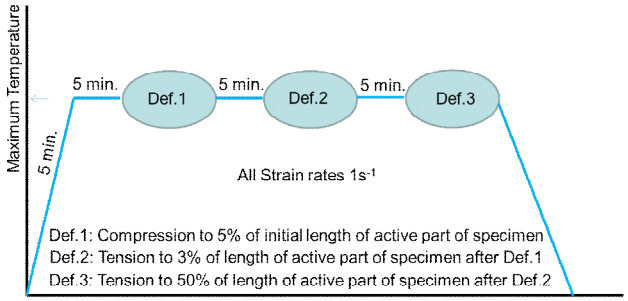

Figure 6: Treatment No. 2

5 RESULTS AND DISCUSSION

5.1 Series A

In order to control the temperature field on the desired material, specimen 1 and 2 were cut by water jet from material 1 sheet and grinded. The results from the thermo camera shown in Figure 7, indicated that the temperature field is stable, continuous and homogenous in the middle part of both specimens with significantly less scaling or even no scale.

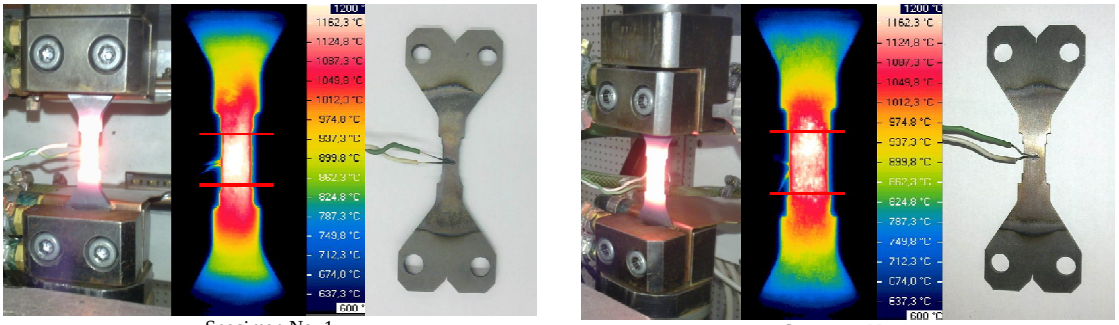

Specimen No. 1 Specimen No. 2

Figure 7: Thermo camera detailed results at 1150ºC (material 1)

5.3 Series B

As a result of test series A, both specimen shapes No. 1 and 2 were tested at three different temperatures, Room Temperature (RT), 750°C and 1150°C via the same treatment (No. 2) as described in section 4. From each deformation, the stress-strain curves were investigated. Figure 8 shows the stress-strain curve for the both specimen shapes No. 1 and 2 during different deformation steps. It can be seen that at 1150ºC, as expected, both specimens shows similar properties and behavior during all deformation steps but as the temperature reduced, two specimens show different reactions in 5% compression and 3% tension. Regarding to the same material on both specimens, this difference could be because of inhomogeneity in the specimen due to inhomogeneity of the mechanically alloyed powder. In this regard, it can be seen that all specimens failed during 50% tension test except specimen 2 at 1150°C. On the other hand, it can be seen that at high temperatures (750°C and 1150°C), both specimens failed around 42% but in RT, they failed around 15%.

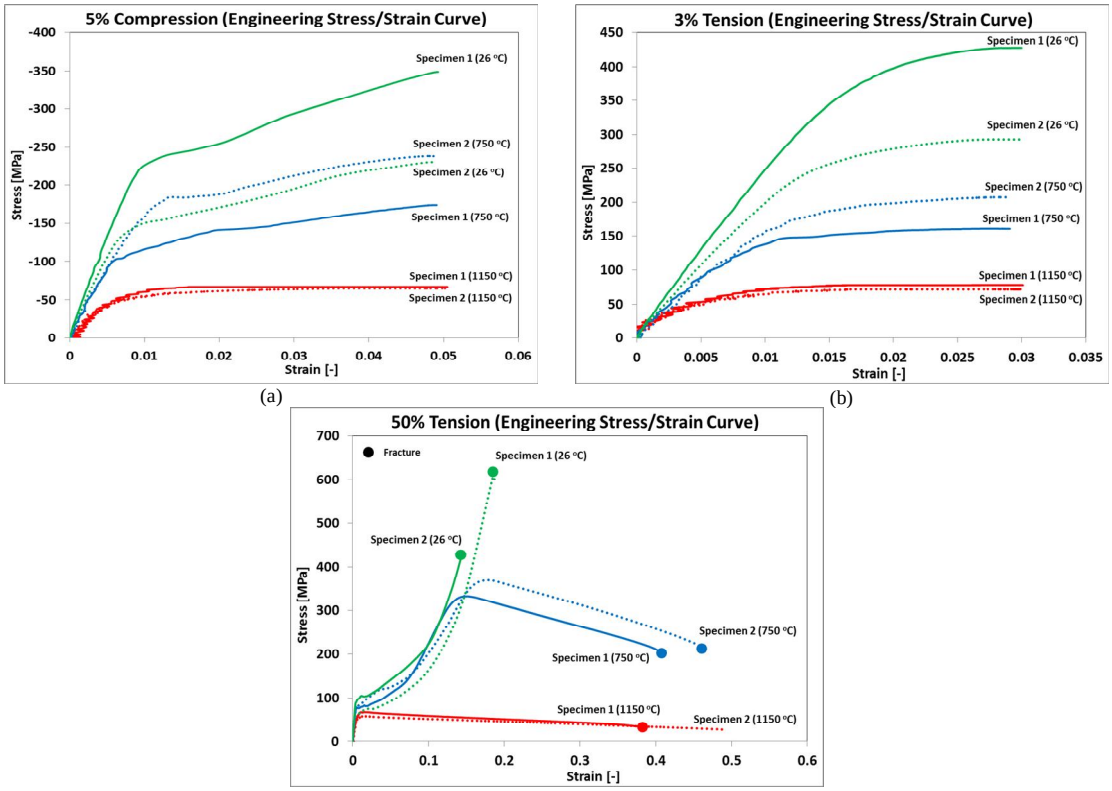

Figure 8: Stress-Strain curves for (a) 5% compression, (b) 3% tension, (c) 50% Tension

5.4 Series C, D, E and F

Test series C to F were carried out in order to investigate the different material behavior under different conditions. Figure 9 shows the stress-strain curves for all materials at different temperatures regarding to the 5% compression of treatment number 2 (figure 6). Material 2 exhibits a better strength at 30°C and 800°C but at 1200°C, material 1 shows a better strength. However the difference between material 2 and 1 strength is acceptable regarding to the high temperature processing. Hot working behavior of alloys is generally reflected on flow curves which are a direct consequence of microstructural changes: the nucleation and growth of new grains, dynamic recrystallization (DRX), the generation of dislocations, work hardening (WH), the rearrangement of dislocations and their dynamic recovery (DRV). In the deformed materials, DRX seems to be the prominent softening mechanisms at high temperatures. DRX occurs during straining of metals at high temperature, characterized by nucleation of low dislocation density grains and their posterior growth to produce a homogeneous grain structure when a dynamic equilibrium is reached.

On the other hand, material 4 showed a strange curve shape at 800 °C. The test was repeated several times and similar results were observed. It could be concluded that it happened because of the inhomogeneity of microstructure of this material.

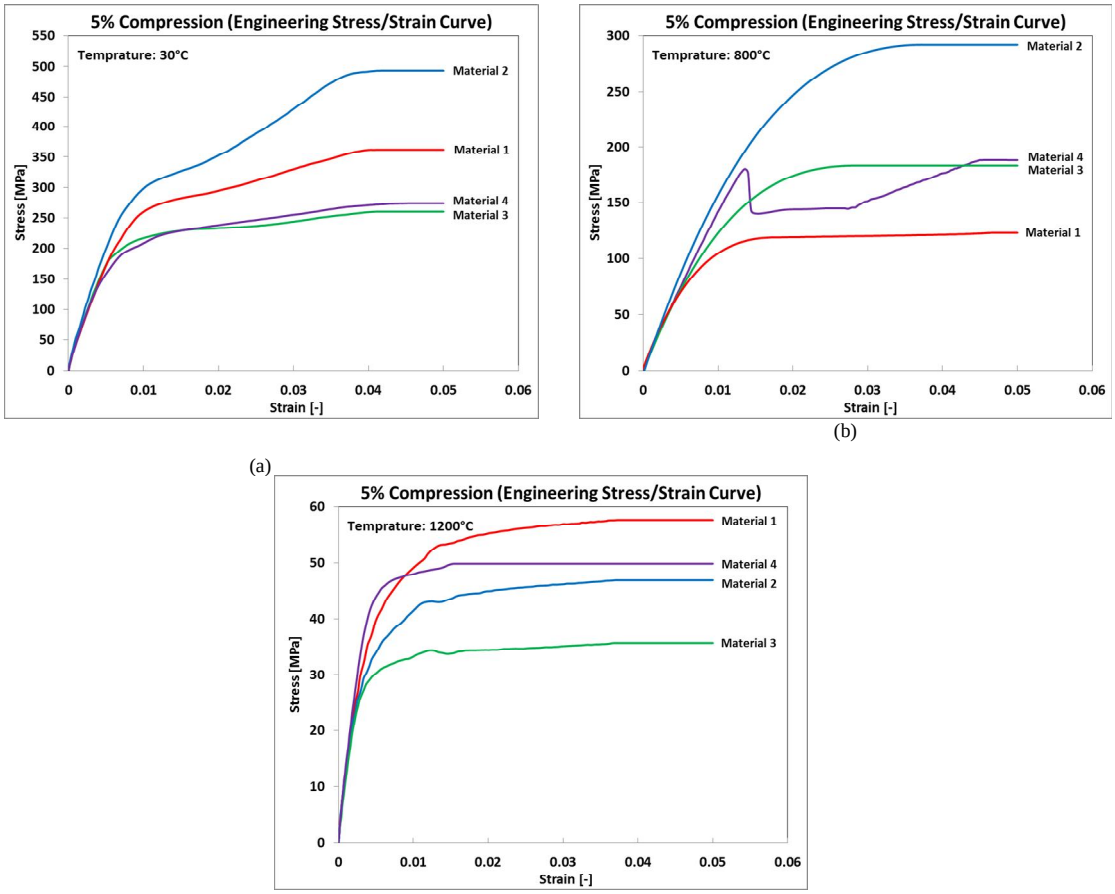

Figure 9: Stress-Strain curves (5% compression) for (a) 30 ^{0}C, (b) 800 ^{0}C, (c) 1200 ^{0}C

Figure 10 shows the stress-strain curves for materials 1 to 4 at different temperatures regarding to the 3% tension of treatment number 2 (figure 6). As it can be seen in figure 10, material 2 shows a higher strength at 30°C and 800°C but at 1200°C, again material 1 shows a better reaction. All four materials has almost similar elastic module and none of them failed during 3% deformation. The yield stress as well as the shape of the flow curves is sensitively dependent on temperature. Comparing all these curves, it is found that decreasing deformation temperature makes the yield stress level increase, in other words, it prevents the occurrence of softening due to dynamic recrystallization (DRX) and dynamic recovery (DRV) and allows the deformed metals exhibiting work hardening (WH). For every curve, after a rapid increase in the stress to a peak value, the flow stress decreases monotonically towards a steady state regime with a varying softening rate which typically indicates the onset of DRX (figure 10c).

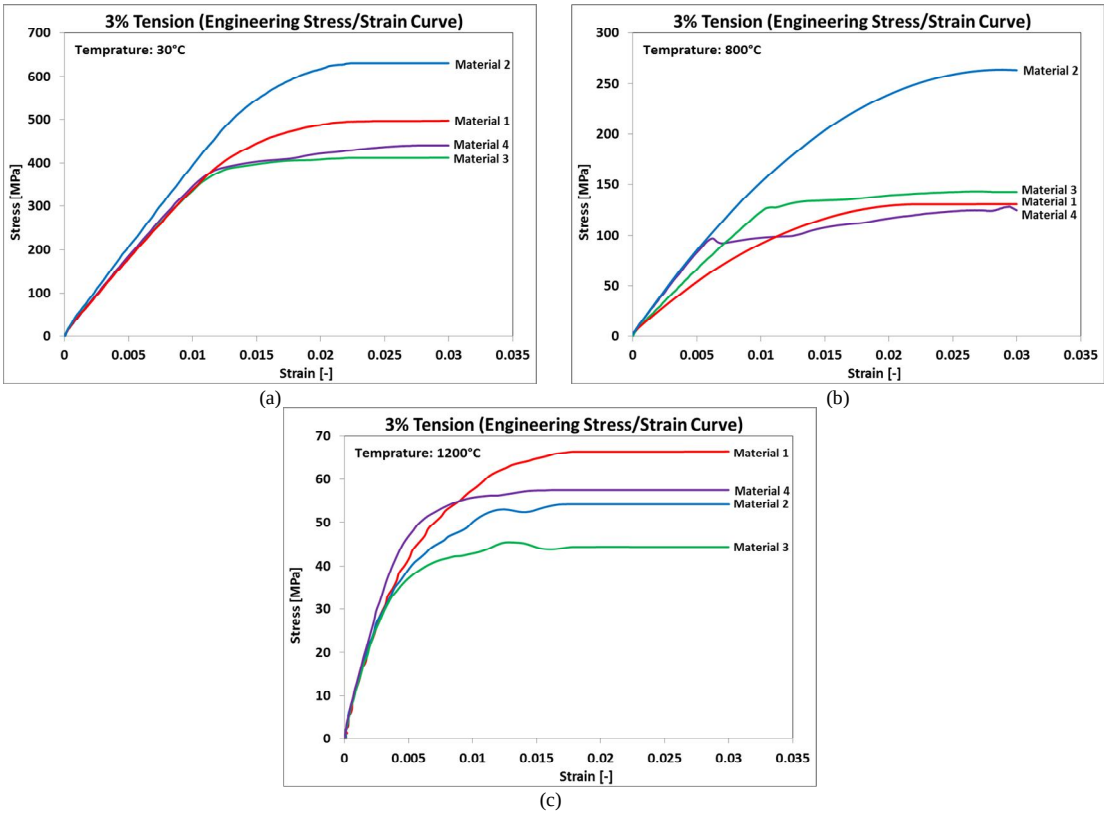

Figure 10: Stress-Strain curves (3% tension) for (a) 30 ^{0}C, (b) 800 ^{0}C, (c) 1200 ^{0}C

Figure 11 shows the stress-strain curves for materials 1 to 4 at different temperatures regarding to the 50% tension of treatment number 2 (figure 6). All 4 materials failed at RT but in higher temperature, only 2 materials failed by 50% tension. From these curves, it also can be seen that the stress evolution with strain exhibits three distinct stages. At the first stage where work hardening (WH) predominates and cause dislocations to polygonize into stable subgrains. Flow stress exhibits a rapid increase to a critical value with increasing strain. Then a large difference in dislocation density within subgrains or grains also grows rapidly and DRX occurs. When the critical driving force of DRX is attained, new grains are nucleated along the grain boundaries, deformation bands and dislocations, resulting in equiaxed DRX grains. At the second stage, flow stress exhibits a smaller and smaller increase until a peak value or an inflection of work-hardening rate. This shows that the thermal softening due to DRX and dynamic recovery (DRV) becomes more and more predominant and it exceeds WH. At the third stage, three types of curve variation tendency can be generalized as following:

1) Decreasing gradually to a steady state with DRX softening (material 3 & 4 in figure 11c),
2) Increasing continuously with significant work-hardening (material 1 & 2 in figure 11b) and
3) Decreasing continuously with significant DRX softening.

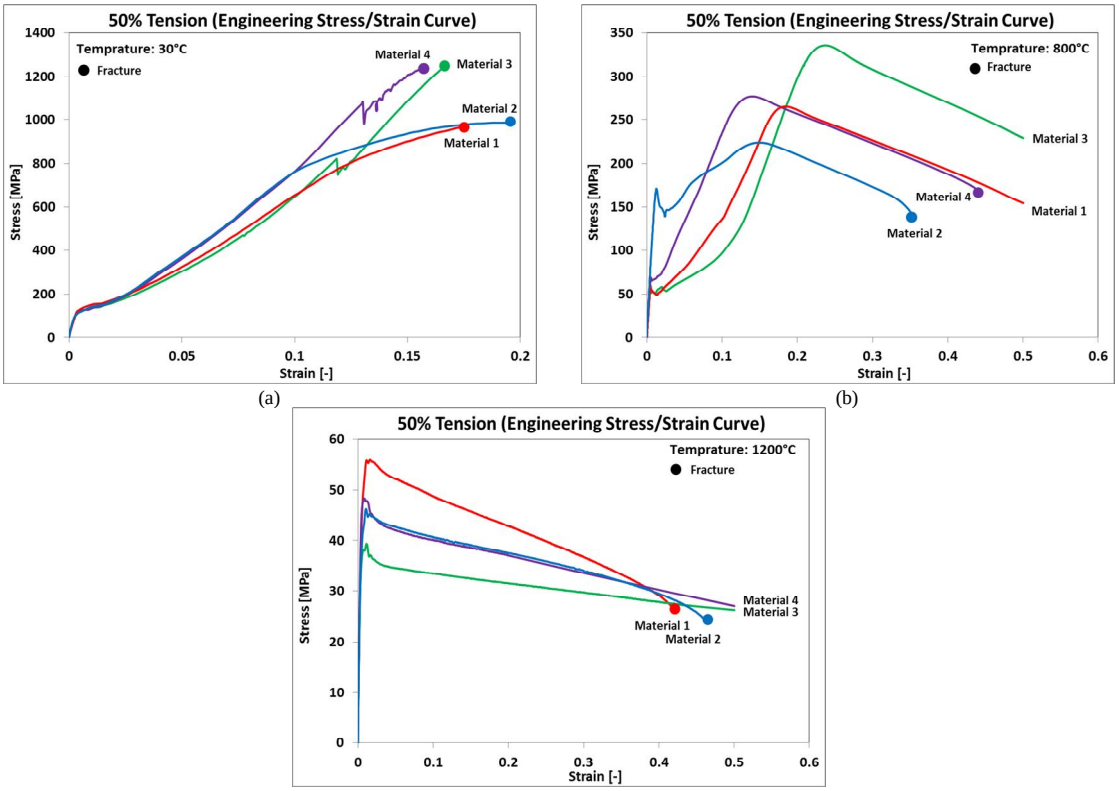

Figure 11: Stress-Strain curves (50% tension) for (a) 30 ^{0}C, (b) 800 ^{0}C, (c) 1200 ^{0}C

6 CONCLUSIONS

This paper outlines the results of characterization of the thermomechanical behaviour of the new generation of ODS alloys and composites. Four materials differing each other in the amount and size of oxides embedded in the ferritic matrix were tested under different conditions. The advantage of all materials is their low-cost and creep- corrosion- and oxidation-resistance due to Fe-Al based ferritic matrix of the ODS alloy. It can be concluded that the typical form of flow curve with DRX softening, including a single peak followed by a steady state flow as a plateau, is more recognizable at high temperatures than at low temperatures. That is because at high temperatures, the DRX softening compensates the WH, and both the peak stress and the onset of steady state flow are therefore shifted to lower strain levels [14]. The characteristics of softening flow behavior coupled with DRX for 4 materials have been discussed and summarized as follows:

1) Decreasing deformation temperature makes the flow stress level to increase, in other words, it prevents the occurrence of softening due to DRX and dynamic recovery (DRV) and makes the deformed metals to exhibit work hardening (WH).

2) For every curve, after a rapid increase in the stress to a peak value, the flow stress decreases monotonically towards a steady state regime (a steady state flow as a plateau due to DRX softening is more recognizable at higher temperatures). A varying softening rate typically indicates the onset of DRX, and the stress evolution with strain exhibits three distinct stages.

3) At higher temperatures, a higher DRX softening compensates the WH, and both the peak stress and the onset of steady state flow are therefore shifted to lower strain levels.

7 ACKNOWLEDGEMENTS

This paper includes results created within the projects 14-24252S Preparation and Optimization of Creep Resistant Submicron-Structured Composite with Fe-Al Matrix and Al2O3 Particles subsidised by the Czech Science Foundation, and LO1502 Development of Regional Technological Institute subsidised by the Ministry of Education, Youth and Sports from specific resources of the state budget of the Czech Republic for research and development.

REFERENCES

[1] *Inco Alloys Limitted, Material data sheet*, INCOLOY, alloy MA 956, INCOLOY, alloy MA 957, Hereford, U.K.
[2] G. Korb, M. Rühle, H.-P. Martinz, *Proceedings of the International Gas Turbine and Aeroengine Congress and Exposition*, Orlando (FL), 3.-6. 7. 1991.
[3] B. Kazimierzak, J.M. Prignon, R.I. *Fromont, Materials and Design* **13**, (1992), 67.
[4] S. Ukai, M. Harada, H. Okada, M. Inoue, S. Nomura, S. Shikakura, T. Nishida, M. Fujiwara, K. Asabe, *J. Nucl. Mat.* **204**, (1993), 74.
[5] R. Schaeublin, T. Leguey, P. Spätig, N. Baluc, M. Victoria, *J. Nucl. Mat*. 307-311, (2002), 778.
[6] *Werkstoffdatenblätter der Fa. PM Hochtemperaturmetall GmbH*, Reutte (A)
[7] F. D. Fischer, J. Svoboda, P. Fratzl, Phil. Mag. 83, (2003), 1075.
[8] J. Rösler, E. Arzt, *Acta Melall.* **38**, (1990), 671.
[9] R. Herzog: Mikrostruktur und Mechanische Eigenschaften der Eisenbasis ODS-Legierungen PM 2000, PhD. Thesis, Forschungszentrum Jülich, Germany, 1997.
[10] K. M. Miller, K. F. Russel, D. T. Hoelzer, *J. Nucl. Materialia*. **351**, (2006), 261.
[11] M. J. Alinger, G. R. Odette, D. T. Hoelzer, *Acta Material*. **57**, (2009), 392.
[12] M. C. Brandes, L. Kovarik, M. K. Miller, G. S. Daehm, M. J. Mills, *Acta Materialia*. **60**, (2012), 1827.
[13] M. C. Brandes, L. Kovarik, M. K. Miller, M. J. Mills, J. Mater. *Sci.* **47**, (2012), 3913.
[14] Guo-Zheng QuanYuan-ping Mao, Gui-sheng Li, Wen-quan Lv, Yang Wang, Jie Zhou. A characterization for the dynamic recrystallization kinetics of as-extruded 7075 aluminum alloy based on true stress-strain curves. *Computational Materials Science*, (2012).
[15] I. Kubena, T. Kruml: Fatigue life and microstructure of ODS steels, *Eng. Fract. Mech*., 2012.
[16] I. Kubena, B. Fournier, T. Kruml: *Journal of Nuclear Materials*, **424** (2012), 101.
[17] B. Fournier, A. Steckmeyer, A.-L. Rouffié, J. Malaplate, J. Garnier, M. Ratti, P. Wident, L. Ziolek, I. Tournié, V. Rabeau, J.M. Gentzbittel, T. Kruml, I. Kubena: *Journal of Nuclear Materials*, **430** (2012), 142.
[18] Palm M., *Intermetallics*, **13** (2005), 1286.
[19] Stein F., Palm M., Sauthoff G., *Intermetallics* **13** (2005), 1275.
[20] Morris D.G., Muñoz-Morris M.A., *Materials Science and Engineering* A **462** (2007), 45.
[21] Jirkova H., Aisman D., Masek B., Svoboda J., *Semi-Solid Processing of Metal–Oxide*

Composite, Proceeding of 23rd international Conference on Metallurgy and Materials (Metal 2014), Brno, Czech Republic
[22] Milenkovic S., Palm M., *Intermetallics* **16** (2008), 1212.
[23] Morris D.G., *Intermetallics* **6** (1998), 753.
[24] Morris-Muñoz MA. *Intermetallics* **7** (1999), 653.
[25] Khalaj O., Masek B., Jirkova H., Ronesova A., Svoboda J., Investigation on New Creep and Oxidation Resistant Materials, *Journal of Materials and Technology,* **52** (2015) 5.
[26] J. Frenzel, A. Wieczorek, I. Opahle, B. Maaß, R. Drautz, G. Eggeler, On the effect of alloy composition on martensite start temperatures and latent heats in Ni–Ti-based shape memory alloys, *Acta Materialia*, **90**, (2015), 213–231.